Jamt.ejournal.unri.ac.id

# Hydrocarbon-Impacted Soils Supported Mn for Organic Pollutant Oxidation



Edy Saputra<sup>1,\*</sup>, Ahmad Fadli<sup>2</sup>, Barata Aditya Prawiranegara<sup>3</sup>, Amun Amri<sup>1</sup>, Desi Helina<sup>1</sup>, Syaiful Bahri<sup>1</sup>, Ari Sandhyavitri<sup>4</sup>, Fajar Restuhadi<sup>5</sup>, Hussein Rasool Abid<sup>6</sup>, Muhammad Rizwan Azhar<sup>7</sup>, Panca Setia Utama<sup>1</sup>

- <sup>1</sup>Department of Chemical Engineering, Riau University, Pekanbaru 28293, Indonesia
- <sup>2</sup>PT Bumi Siak Pusako, Dayun, Siak Sri Indrapura, Riau, Indonesia
- <sup>3</sup>Department of Chemistry, Faculty of Mathematics and Natural Sciences, Universitas Riau, Pekanbaru, Indonesia
- <sup>4</sup>Department of Civil Engineering, University of Riau, Pekanbaru, Indonesia
- <sup>5</sup>Faculty of Agriculture, University of Riau, Pekanbaru, Indonesia
- <sup>6</sup>Environmental Health Department, College of Medical Sciences, University of Kerbala, Karbala, Iraq.
- Mineral Resource Recovery Center, School of Engineering, Edith Cowan University 270 Joondalup Drive Joondalup 6027

ABSTRACT: Hydrocarbon-impeded soil (HIS) is solid waste from spills or leaks during industrial activities that negatively impact the environment. This study aims to utilize HIS as catalyst support on MnO<sub>2</sub> to degrade RhB (RhB) solution using Peroxymonosulfate (PMS) and to determine the optimum conditions for the catalyst to degrade RhB. The catalyst was synthesized by reacting HIS, calcined with KMnO4 with various catalyst supports with high and low Total contain Petroleum Hydrocarbon (TPH). The process degradation of Rhodamine Solution was carried out with various catalysts, PMS, and RhB concentrations. The catalyst was characterized using X-ray diffraction (XRD), Nitrogen gas adsorption-desorption (BET), and Scanning Electron Microscope-Energy Disperse Spectroscope (SEM-EDX). In this study, the best catalyst performance was MnO<sub>2</sub>@H-TPH, which could activate PMS to degrade RhB with dye removal of 98% in about 180 min, at conditions 10 g/L RhB, 0.1 g/L catalyst, and 3 g/L PMS with the activation energy of 16.3 kJ/mol.

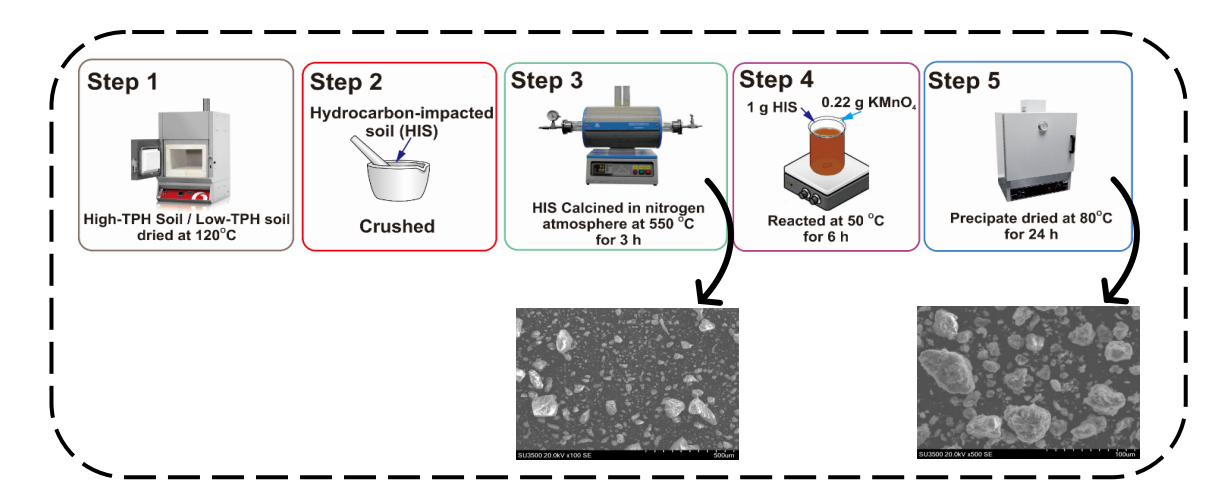
Key words: Crude oil contaminated soil, Mn catalyst, dye degradation, peroxymonosulfate, wastewater treatment

#### 1. INTRODUCTION

Currently, many industries produce waste that causes environmental pollution. The waste could be solid, liquid, or gas form. Hydrocarbon-impacted soil (HIS) is solid waste originating from petroleum due to accidental spills or leaks that occur during industrial activities [1]. HIS can cause harmful effects on microbes, animals, and plants. Soil contaminated below 1% will inhibit bacteria in the soil. Soil containing 3% oil will cause worms in the soil for more than 7 days, and oil contamination also hampers plant growth [2] [2, 3]. One way to treat soil contaminated with petroleum is through bioremediation by adding microbes with a high potential to degrade petroleum hydrocarbon [3]. According to Oluremi & Osualale [4], contaminated soil can be used as construction material, including subgrade material in road construction, brick and tile production, concrete mixes, and production of asphalt concrete.

Liquid waste from industries and households contains many organic components that harm the environment and living things. Liquid waste treatment that is often carried out includes biodegradation, electrocoagulation, adsorption with activated carbon, and the Advanced Oxidation Process (AOP). Among these methods, the AOP method is effective and efficient, using highly reactive active radicals to remove pollutants found in water [5]. One active radical used in the AOP is sulfate radical (SO4 -), which can be used to replace the hydroxyl radicals because it has an oxidation potential of 1,82 V greater than H<sub>2</sub>O<sub>2</sub>, which has an oxidation potential of 1,76 V [6]. PMS can be activated using external activator energy such as ultrasonic, heat, and ultraviolet, metal ions (Ni<sup>2+</sup>, Fe<sup>3+</sup>, Mn<sup>2+</sup>), and chemicals such as alkaline compounds, phenol, and quinone [7, 8]. Using carbonbased catalysts also increases persulfate's ability to degrade pollutants, and the carbonyl group plays an essential role in the composition of persulfate into  $SO_4^{*-}$ . Another advantage of carbon materials is that they can actively persulfate at neutral pH without using additional energy and chemicals [9, 10].

Received : December 20, 2023
Revised : December 13, 2023
Accepted : December 2, 2023



**Scheme 1.** The diagram of the preparation for catalysts.

Previous researchers have widely applied the advanced oxidation process (AOP) using a carbon manganese composite-based catalyst as an oxidizing agent. Organic content in HIS will reduce the manganese compound in KMnO<sub>4</sub> to produce active manganese oxide and carbon composite for the AOP catalyst. Carbon in the catalyst matrix also provides additional active catalytic sites for the AOP process [11]. Prawiranegara et al. [12] synthesized Mn/Carbon using manganese nitrate with a carbon source from glucose and degraded methylene blue solution at a concentration of 25 mg/L using peroxymonosulfate. Wang et al. [13] have succeeded in synthesizing Mn/MCS catalysts and carrying out phenol degradation at a concentration of 20 mg/L with peroxymonosulfate. Phenol was degraded using Mn/Air-MCS, and the Mn/N2-mcs catalyst reached 100% within 120 minutes. Yan et al. [14] have succeeded in synthesizing CNT/MnO2 by reducing Pottasium Permanganate using CNTs. CNT/MnO2 is used as high-power, high-density supercapacitors. Prawiranegara et al. [12] synthesized Mn/Carbon using Manganese Nitrate with a carbon source from glucose and degraded methylene blue solution at a concentration of 25 mg/L using peroxymonosulfate.

In this study, RhB solution was treated using the AOP method to produce sulfate radicals. HIS will be used as catalyst support, reacting with Pottasium Permanganate. The catalyst obtained will activate Peroxymonosulfate (PMS) to degrade RhB. The use of HIS is an effort to develop the utilization of toxic and hazardous waste that is harmful to the environment.

#### 2. EXPERIMENTAL

# 2.1 Material and Catalyst Preparation

Hydrocarbon-impacted soil (HIS) was obtained from an oil field exploration in Riau province, Indonesia, and was utilized without further treatment. RhB (C<sub>28</sub>H<sub>31</sub>ClN<sub>2</sub>O<sub>3</sub>) and potassium permanganate (KMnO<sub>4</sub>) were obtained from Merck, respectively. For peroxymonosulfate, PMS (2KHSO<sub>5</sub>.KHSO<sub>4</sub>.K<sub>2</sub>SO<sub>4</sub>) was obtained from Sigma Aldrich.

HIS as a supported catalyst was prepared from two different total petroleum hydrocarbons (TPH) contained in the soil, namely high-TPH (H-TPH) and low-TPH (L-TPH). Firstly, HIS will be dried at 120°C for 24 h and crushed into particles as pretreatment. The particles were calcinated in nitrogen using a tubular furnace with a temperature of 550°C for 3 hours, and then the calcinated contaminated soil was cooled using a desiccator. A fixed amount of 1 g calcinated HIS reacted with 0.22 g potassium permanganate. The mixture dissolved with 100 mL aquadest, heated using a water batch at 50°C, and stirred for 6 hours. The precipitate was washed with aquades three times. The precipitate dried in an oven at 80°C for 24 hours. The obtained catalysts were denoted MnO<sub>2</sub>@H-TPH and MnO<sub>2</sub>@L-TPH. The synthesis of the catalyst is presented in Scheme 1.

#### 2.2 Characterization

The crystalline structure of supported catalysts (L- and H-TPH) and catalysts (MnO<sub>2</sub>@L and MnO<sub>2</sub>@H-TPH) were analyzed by XRD (*X-ray Diffraction*, Bruker D8 advanced equipped with a Lynx eye detector, Bruker-AXS, Germany) operated at 40 kV and 30 mA. Nitrogen sorption isothermal analysis (NOVA 4200e, Quantachrome) for Brunauer-Emmett-Teller (BET) analysis to determine the specific surface area and pore volume. Catalyst morphology was determined using Field

Emission Scanning Electron Microscope (FESEM) (JEOL Type JIB4610F). The morphologies of the catalyst were observed using the field scanning electron microscope (A JEOL JSM-6300F, USA). EDS, energy-dispersive X-ray spectroscopy were also utilized to detect metal particles on supported catalysts. TPH contained in the soil was measured by GC with a flame ionization detector (FID).

#### 2.3 Oxidation Processes

The dye used was RhB (RhB) with various concentrations (5, 10, 20, and 50 mg/L) in a beaker with a volume of 500 mL. The solution was added to Peroxymonosulfate (PMS) with various concentrations

(0.5, 1, 2, and 3 g/L), then added to the catalyst with various concentrations (0.05, 0.1, 0.2, 0.4 g/L). The degradation was done for 180 minutes with a stirring speed of 400 rpm. Sampling was performed every 15 minutes and centrifuged (3000 rpm for 2 min). The absorbance value of the solution was measured using a UV-VIS spectrophotometer.

#### 3. RESULT AND DISCUSSION

#### 3.1 Characterization of the Catalyst

The composition and some properties of the received HIS are listed in Table 1. As can be seen, the support material consists mainly of silica and aluminum and has slight differences in calcium, magnesium, and potassium due to the different soil sources.

**Table 1** Composition and properties of supported and catalysts.

| Component  | L-TPH<br>(wt%) | H-TPH<br>(wt%) | MnO <sub>2</sub> @L-<br>TPH<br>(wt%) | MnO <sub>2</sub> @<br>H-TPH<br>(wt%) |
|--|----------------|----------------|--------------------------------------|--------------------------------------|
| Carbon (C)   | 18.22          | 55.54          | 18.06                                | 21.39                                |
| Silica (Si)  | 51.21          | 22.27          | 48.36                                | 28.26                                |
| Aluminum<br>(Al)   | 29.59          | 18.17          | 31.36                                | 23.82                                |
| Iron (Fe)  | 0.98           | 1.38           | 0.62                                 | 1.97                                 |
| Calcium (Ca)   | -              | 0.74           | -                                    | 0.95                                 |
| $\begin{array}{c} {\sf Magnesium} \\ {\sf (Mg)} \end{array}$ | -              | 0.36           | -                                    | 0.35                                 |
| Manganese<br>(Mn)  | -              | -              | 1.60                                 | 20.02                                |
| Potassium<br>(K)   | -              | 1.54           | -                                    | 3.24                                 |

Fig. 1 shows XRD patterns of L-TPH and H-TPH and their supported Mn catalysts. The predominant phase for support is quartz and mullite with minor iron, calcium, magnesium, nickel, and potassium. After KMnO<sub>4</sub> reacted with both HIS, only one peak was observed at 20 28.85°, corresponding to the diffractions of MnO<sub>2</sub> (JCPDS No. 50-0866, a = 4.437 A), possibly because of fine particles and high dispersion [15]. The surface area and pore volume of the support and catalyst were determined using the N2 adsorption-desorption method shown in Fig. 2. MnO<sub>2</sub>@H-TPH has a higher surface area and pore volume (149.5 m<sup>2</sup>/g and 0.208 cm<sup>3</sup>/g) than others, while L-TPH has the lowest surface area and pore volume. Furthermore, all catalysts have pore radius between 20 Å and 200 Å, which means they are mesoporous and macroporous materials. The support and catalyst were identified as type IV isotherms with material properties that have pores [16]. The surface area and pore size of the catalyst and support can be seen in Table 2.

SEM micrographs and EDS spectra of  $MnO_2@L$ -TPH and  $MnO_2@H$ -TPH, as well as Mn and other metals elemental mapping, are shown in Fig. 3 and 4. Both catalysts have an irregular shape with a particle size of 0.5  $\mu$ m15  $\mu$ m

(Fig. 3a and 4a). Some spherical-like particles are also evident. EDS measurement displays the presence of elements, as shown in Table 1, Fig. 3b and 4b. The catalyst supports, namely Low TPH (L-TPH) and High TPH (H-TPH), do not have the Mn element in their component constituent (Table 1). HIS reacted with KMnO<sub>4</sub>, resulting in the MnO<sub>2</sub>@HIS catalyst having the element Mn. The estimated Mn contents for MnO<sub>2</sub>@L-TPH and MnO<sub>2</sub>@H-TPH were 1.6 and 20 wt%, respectively. According to characterization, MnO<sub>2</sub>, as the significant Mn species, was present on the surface of the Mn catalyst, and MnO<sub>2</sub>@H-TPH showed a better Mn dispersion. Moreover, it was discovered that Mn revealed a superior dispersion on MnO<sub>2</sub>@H-TPH than MnO<sub>2</sub>@L-TPH.

Table 2 Surface area, pore volume, and pore radius of catalyst.

| Catalyst                    | $S_{BET}(m^2/g)$ | Pore Volume<br>(V, cm <sup>3</sup> /g) | Average Pore<br>Radius (Å) |
|-----------------------------|------------------|--|----------------------------|
| L-TPH                       | 9.61             | 0.098                                  | 205.32                     |
| H-TPH                       | 16.38            | 0.106                                  | 129.90                     |
| MnO₂@L-<br>TPH              | 134.90           | 0.196                                  | 29.12                      |
| MnO <sub>2</sub> @H-<br>TPH | 149.50           | 0.208                                  | 27.85                      |

#### 3.2 The Effect of the Different Catalyst

Fig. 5 shows the degradation of RhB concentration with various catalysts as a function of time. MnO<sub>2</sub>@H-TPH exhibited low adsorption of RhB at approximately 3%, while PMS without catalyst provided RhB removal of approximately 18% in 180 min. It was revealed that H-TPH moderately activated PMS to produce sulfate radicals, with RhB removal of about 21%. MnO<sub>2</sub>@L-TPH with PMS can degrade RhB up to 39% in 180 min, while at the same time duration, MnO<sub>2</sub>@H-TPH can reach 80.84% RhB removal. For hydrocarbon-impacted soil containing high carbon (Table 1), KMnO4 could form more MnO<sub>2</sub> than those containing low carbon, resulting in a high efficiency of RhB degradation. The reaction between KMnO<sub>4</sub> and Carbon follows the redox reaction below.

$$MnO_4^- + 4H^+ + 3e^- \rightarrow MnO_2 + 2H_2O$$
 (1)

$$2C + 4OH^{-} \rightarrow 2C^{+} + 2H_{2}O + O_{2} + 4e^{-}$$
 (2)

$$2C^+ + 2e^- \rightarrow 2C \tag{3}$$

The manganese (Mn) content in the two samples had different percentage values that contributed to PMS activation. The reactions during the degradation process are as follows [17].

$$HSO_5^- + 2MnO_2 \rightarrow Mn_2O_3 + SO_5^- + OH^-$$
 (4)

$$HSO_5^- + Mn_2O_3 \rightarrow 2MnO_2 + SO_4^- + H^+$$
 (5)

$$SO_4^{-} + H_2O \rightarrow SO_4^{2^-} + OH + H^+$$
 (6)

RhB + 
$$SO_4$$
  $\rightarrow$  [several steps]<sub>n</sub>  $\rightarrow$   $CO_2$  +  $H_2O$  +  $SO_4$ <sup>2</sup> (7)

RhB + 
$$SO_5^{-}$$
  $\rightarrow$  [several steps]<sub>n</sub>  $\rightarrow$   $CO_2$  +  $H_2O$  +  $SO_4^{2}$  (8)

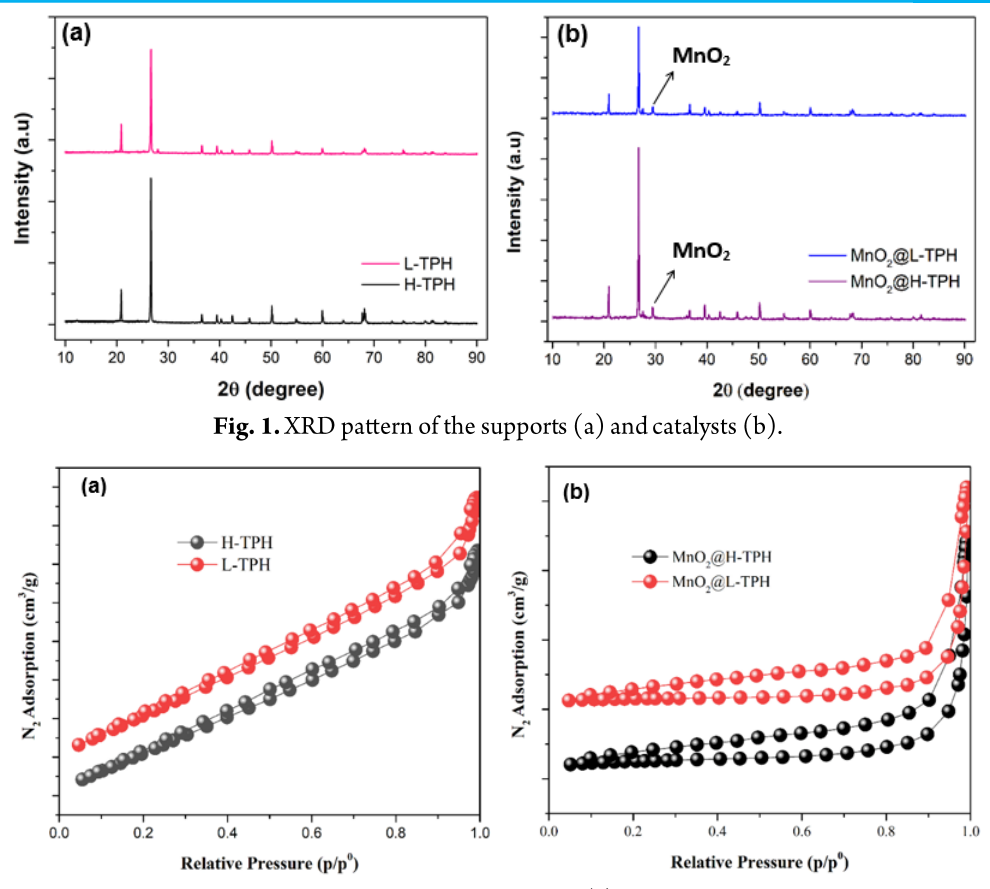
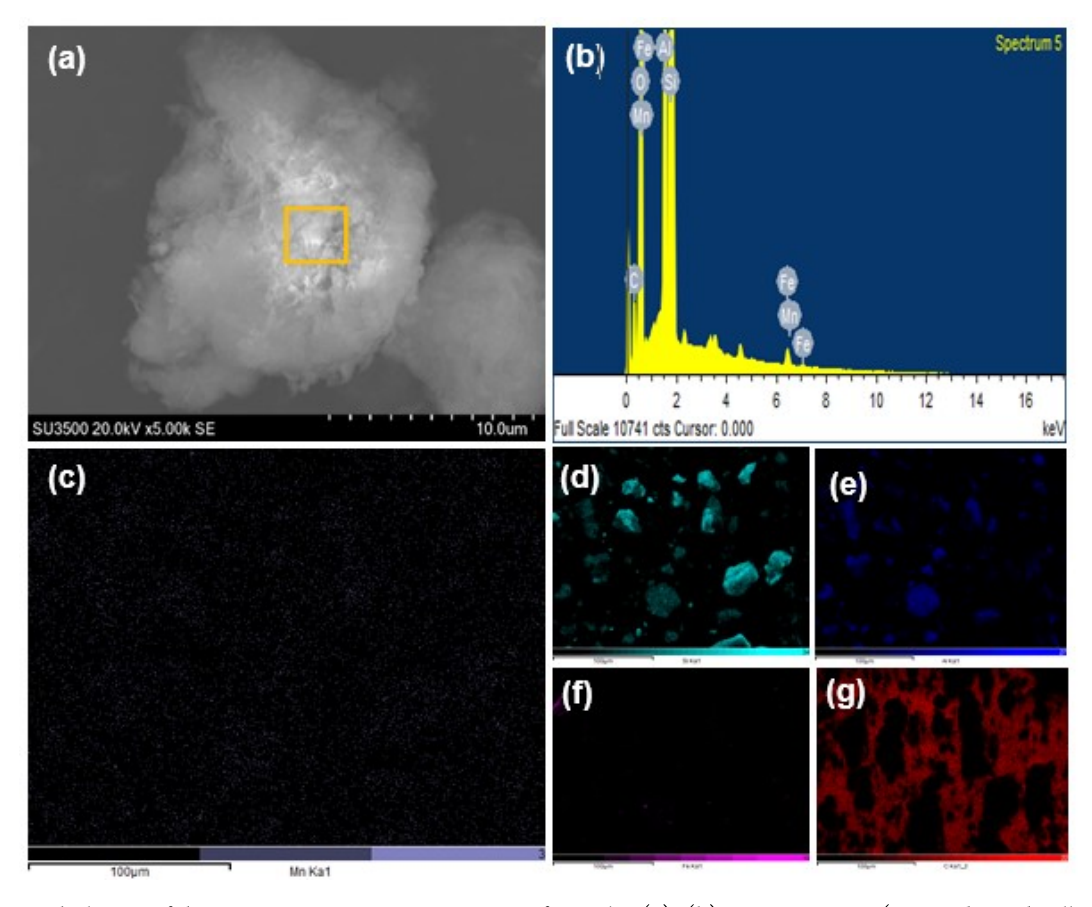
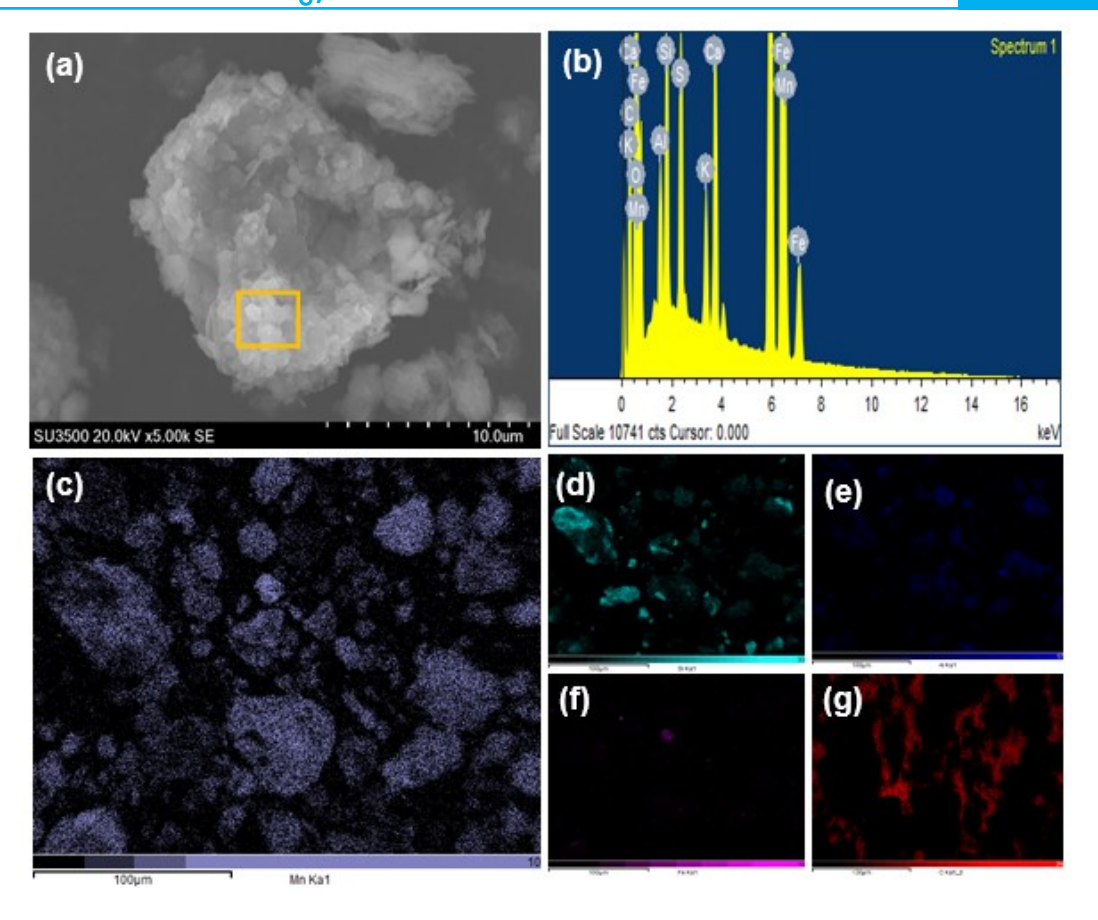


Fig. 2. N<sub>2</sub> Adsorption-desorption isotherms of L-TPH and H-TPH (a) and MnO<sub>2</sub>@L-TPH and MnO<sub>2</sub>@H-TPH (b).

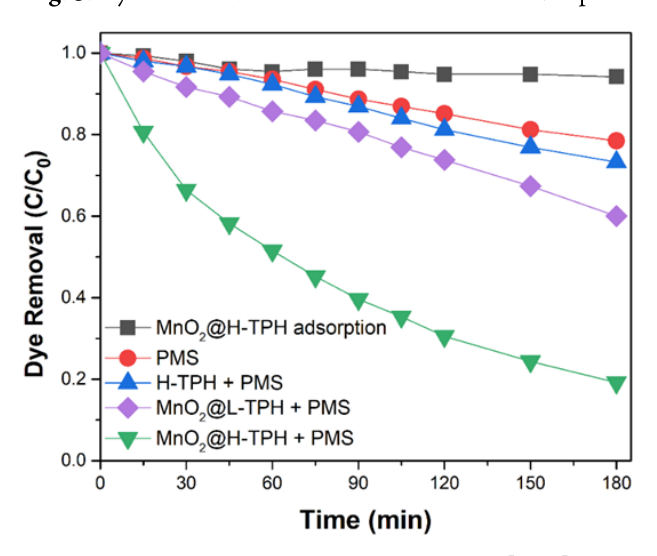


**Fig. 3.** Morphologies of the  $MnO_2@L$ -TPH . SEM images of samples (a), (b) EDS spectrum (area indicated yellow frame), and the elemental mapping images (c) Mn, (d) Si, (e) Al, (f) Fe and (g) C.



**Fig. 4.** Morphologies of the MnO<sub>2</sub>@L-TPH . SEM images of samples (a), (b) EDS spectrum (area indicated yellow frame), and the elemental mapping images (c) Mn, (d) Si, (e) Al, (f) Fe and (g) C.

Fig. 5. Dye removal of RhB removal with time in adsorption



and catalytic oxidation. Reaction conditions: [RhB] = 10 mg/L; [catalyst] = 0.1 g/L; [PMS] = 2 g/L; T =  $30^{\circ}$ C.

Saputra et al. [18, 19, 20] investigated the removal of phenol by activating PMS heterogeneously through the use of synthesis Mn oxides. They reveal that  $MnO_2$  is responsible for PMS activation. Some other investigations using MnOx/SBA-15 to target anti-biodegradation drugs have been done

by Yang et al. [21]. They discovered that the surface electron relocation between triple bond  $\mathrm{MnO_x(OH)_y}$  species of  $\mathrm{MnOx/SBA-15}$  and  $\mathrm{HSO_5}^-$  of PMS was reliable for developing reactive oxygen radicals, thus promoting ibuprofen degradation. Saputra et al. [22] studied the removal of palm oil mill secondary effluent by activating PMS through  $\mathrm{LaMnO_3}$  perovskite. They found that  $\mathrm{Mn(IV)}$  is responsible for PMS activation. Hence, it is seen that  $\mathrm{MnO_2@H-TPH}$  in this study with PMS has a similar consequence in which  $\mathrm{SO_4}^-$  and  $\mathrm{SO_5}^-$  are critical roles for dye removal. It was concluded that the  $\mathrm{MnO_2@H-TPH}$  system was cheaper than the abovementioned one. Due to  $\mathrm{MnO_2@H-TPH}$ 's high performance, further tests on  $\mathrm{MnO_2@H-TPH}$  were conducted to understand the impact of operating conditions.

#### 3.3 The Effect of the Different Concentration Catalyst

The removal of RhB as a result of catalyst loading is observed in Fig. 6. The catalyst concentration was varied with a range of 0.05 to 0.4 g/L to determine the optimum mass concentration of the best catalyst. The degradation process was done using a solution of 10 mg/L RhB and 2 g/L PMS in 180 min. It shows that increasing the amount of catalyst in the solution causes the efficiency of RhB degradation to be more significant.

As the loading of MnO<sub>2</sub>@H-TPH was 0.05 g/L, the RhB degradation efficiency was 59%. It further increased the catalyst to 0.1 g/L, and the removal efficiency increased to 80.84%. However, for catalyst loading 0.2 and 0.4 g/L, the RhB degradation efficiency remains relatively stable after 180 min, at 76% and 81.43%, respectively. This indicates that  $SO_4$  and  $SO_5$  radicals were not increased to remove dye due to the amount of PMS being the same during the reaction [23, 24]. This suggests that for MnO<sub>2</sub>@H-TPH, the optimum catalyst concentration was 0.1 g/L because the catalyst loading of 0.4 g/L has a relatively similar efficiency value.

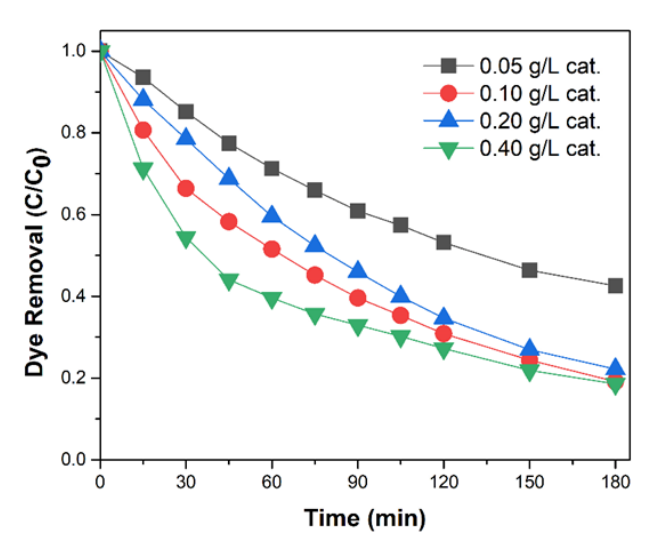


**Fig. 6**. Effect of catalyst concentration on the degradation of RhB. Reaction conditions: [RhB] = 10 mg/L; [PMS] = 2 g/L; reaction temperature = 30°C.

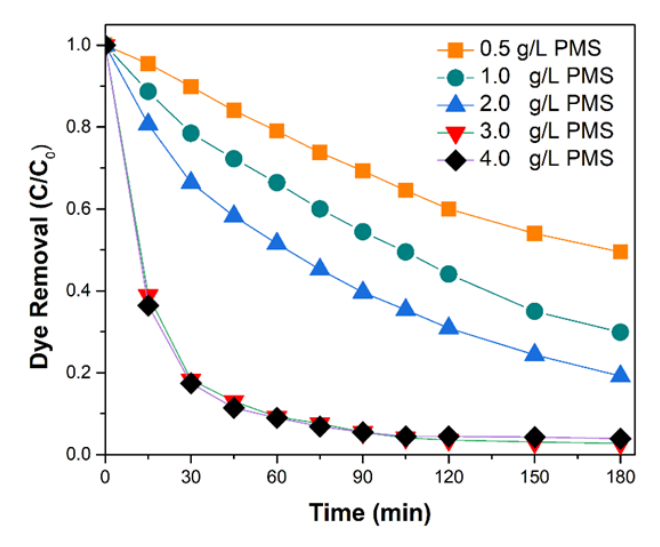
#### 3.4 The Effect of the Different Concentration PMS

Based on Fig. 7 adding PMS concentration significantly affects the dye removal of RhB degradation. As can be seen, Increasing the PMS concentration used will increase the amount of sulfate radicals formed. The highest degradation of RhB can be achieved at 98% with 3 g/L PMS in 180 min. However, more PMS added will reduce dye removal efficiency due to inhibition, resulting in the formation of  $\mathrm{SO_5}^{-1}$ , which is less effective than  $\mathrm{SO_4}^{-1}$  [25].

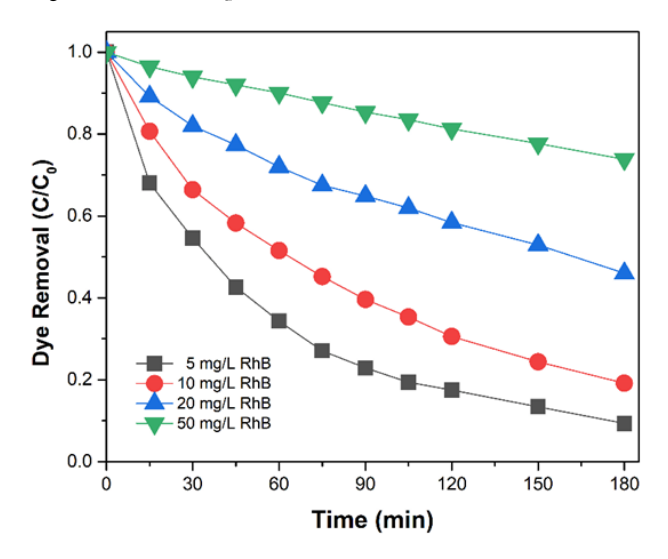
#### 3.5 The Effect of the Different Concentration RhB

Fig. 8 shows that the difference in RhB concentration affects dye removal efficiency. RhB concentrations were varied with a 5-50 mg/L concentration range to determine the effect on dye removal. The rate of removal was slower with increasing concentrations of RhB. 90.6% degradation efficiency of RhB was achieved within 180 min at RhB concentration of 5 mg/L, while in the same duration of time at RhB concentrations of 10, 20, and 50 mg/L, removal efficiency 80.84%, 55%, and 20.5%, respectively. For various RhB concentrations, the removal efficiency is conditional on sulfate radicals. Due to the same concentrations of MnO<sub>2</sub>@H-TPH and PMS, the sulfate radical concentration produced in the solution will be the same. Therefore, a high concentration of RhB in solution will require more time to

obtain the same removal rate, thus reducing RhB degradation efficiency [17, 26].



**Fig. 7**. Effect of PMS concentration on the degradation of RhB. Reaction Conditions: [catalyst] = 0.1 g/L; [RhB] = 10 mg/L; reaction temperature =  $30^{\circ}$ C.



**Fig. 8.** RhB degradation with various concentrations. Reaction conditions: [catalyst] = 0.1 g/L; [PMS] = 2 g/L; reaction temperature =  $30^{\circ}$ C.

# 3.6 The Effect of the Temperature on RhB Degradation

The temperature significantly affects chemical reactions because of the energy involved in the overall process, as illustrated in Fig. 9. It shows that a higher temperature in the degradation of RhB will generally increase the reaction rate [12, 27]. At a temperature of 30°C, RhB degradation would reach 80.84% at 10 mg/L in 180 min. For the temperature of 40 and 50°C, RhB degradation efficiency were achieved at 89 and 91.5%, respectively. In order to predict the kinetic rates, a general pseudo-first-order kinetics for RhB removal was employed, as shown in the equation below.

$$\operatorname{Ln}\left({^{C}/_{C_0}}\right) = -k_{obs} \cdot t \tag{6}$$

Where  $k_{obs}$  is the apparent first-order rate constant of RhB degradation, and C is the concentration of RhB at different times (t).  $C_0$  is the initial RhB concentration. Fig. 9 shows that the degradation of RhB followed the first-order kinetics, and the rate of constants of the MnO<sub>2</sub>@H-TPH are displayed in Table 3. Herein, the  $k_{obs}$  is increased as the temperature increases.

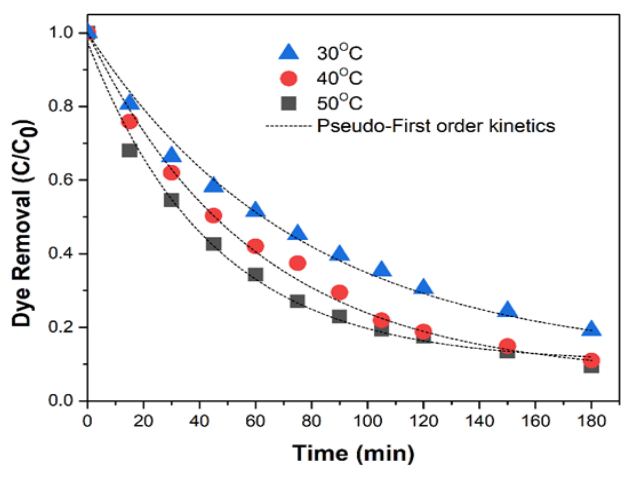


**Fig. 9.** RhB degradation with various reaction temperatures. Reaction conditions: [catalyst] = 0.1 g/L; [PMS] = 2 g/L; [RhB] = 10 mg/L.

**Table 3** First-order rate constant of RhB degradation (k<sub>obs</sub>) on MnO<sub>2</sub>@H-TPH.

| Temperature (°C) | $k_{obs}$ | Activation energy (kJ mol <sup>-1</sup> ) |
|------------------|-----------|---|
| 30               | 0.0098    |   |
| 40               | 0.0123    | 16.3                                      |
| 50               | 0.0146    |   |

The activation energy of  $MnO_2@H\text{-}TPH$  is obtained using the Arrhenius plot of the rate constant and temperature of the reaction. The activation energy of  $MnO_2@H\text{-}TPH$  is estimated at around 16.3 kJ/mol. The activation energy is relatively low compared to the other materials, such as cobalt-based tourmaline/ $La_1^-_xCe_xCoO_3$  (46.6kJ/mol), Fe-Co layered double hydroxide (FeCo-LDH) (59.71 kJ/mol), and  $LaMnO_3$  perovskite (45.5 kJ/mol). The comparison is presented in Table 4.

**Table 4** Activation energy of various catalysts in AOP reactions.

| Catalyst   | Activation energy (kJ/mol) | Ref       |
|--|----------------------------|-----------|
| Tourmaline/<br>La <sub>1</sub> - <sub>x</sub> Ce <sub>x</sub> CoO <sub>3</sub> | 46.60                      | [28]      |
| Fe-Co layered double<br>hydroxide (FeCo-LDH)                                   | 59.71                      | [29]      |
| LaMnO <sub>3</sub> perovskite  | 45.50                      | [22]      |
| Carbon aerogel   | 22.11                      | [30]      |
| MnO <sub>2</sub> @H-TPH  | 16.30                      | This work |

#### 4. Conclusion

MnO $_2$ @H-TPH catalyst has been successfully synthesized using hydrocarbon-impacted soil reacted with KMnO $_4$ . The synthesized catalyst was used to degrade the Rhodamine solution using PMS based on the AOP method. Optimum results were obtained in degraded RhB solution (10 mg/L) using MnO $_2$ @H-TPH with dye removal of 98% using a catalyst with a concentration of 0,1 g/L and PMS concentration of 3 g/L for 180 minutes. RhB degradation reaction is described as a pseudo-first-order reaction with the activation energy of MnO $_2$ @H-TPH of 16.3 kJ/mol. Synthesized MnO $_2$ @HIS is expected to be one of the ways to utilize hydrocarbon-impacted soil, making it a promising alternative for utilizing hydrocarbon-impeded soil.

### AUTHOR INFROMATION

## **Corresponding Author**

\*Email: edysaputra@unri.ac.id

#### ORCID (D)

 Edy Saputra
 : 0000-0001-6430-9072

 Barata Aditya Prawiranegara
 : 0000-0001-6430-9072

 Amun Amri
 : 0000-0001-8896-6405

 Ari Sandhyavitri
 : 0000-0002-3174-5502

 Fajar Restuhadi
 : 0000-0003-2560-7936

 Hussein Rasool Abid
 : 0000-0003-3368-371X

 Muhammad Rizwan Azhar
 : 0000-0002-5938-282X

 Panca Setia Utama
 : 0000-0002-6829-1321

# ACKNOWLEDGEMENTS

This project was supported by the Indonesian Ministry of Research, Technology, and Higher Education (Ristekdikti) and PT Bumi Siak Pusako.

#### REFERENCES

- [1] Hassan HF, Taha R, Al Rawas A, Al Shandoudi B, Al Gheithi K, Al Barami AM. Potential uses of petroleum-contaminated soil in highway construction. Construction and Building Materials. 2005;19(8):646-52.
- [2] Chen J, Hu Z, Zhu M, editors. Review on catalytic oxidation degradation of oil-contaminated soil by Fenton-like reagent. IOP Conference Series: Earth and Environmental Science; 2019: IOP Publishing.
- [3] Larasati TRD, Mulyana N. Bioremediasi lahan tercemar limbah lumpur minyak menggunakan campuran bulking agents yang diperkaya konsorsia mikroba berbasis kompos iradiasi. Jurnal Ilmiah Aplikasi Isotop dan Radiasi. 2016;9(2).
- [4] Oluremi JR, Osuolale OM. Oil contaminated soil as potential applicable material in civil engineering construction. Journal of Environment and Earth Science. 2014;4(10):87-99.

- [5] Ahmed Y, Yaakob Z, Akhtar P. Degradation and mineralization of methylene blue using a heterogeneous photo-Fenton catalyst under visible and solar light irradiation. Catalysis Science & Technology. 2016;6(4):1222-32.
- [6] Saputra E, Muhammad S, Sun H, Ang H-M, Tadé MO, Wang S. Shape-controlled activation of peroxymonosulfate by single crystal α-Mn2O3 for catalytic phenol degradation in aqueous solution. Applied Catalysis B: Environmental. 2014;154:246-51.
- [7] Xiao P-f, An L, Wu D-d. The use of carbon materials in persulfate-based advanced oxidation processes: A review. New Carbon Materials. 2020;35(6):667-83.
- [8] Sun X, editor An Overview of Advanced Oxidation Process and Outlook. IOP Conference Series: Earth and Environmental Science; 2022: IOP Publishing.
- [9] Zhao Q, Mao Q, Zhou Y, Wei J, Liu X, Yang J, et al. Metal-free carbon materials-catalyzed sulfate radical-based advanced oxidation processes: a review on heterogeneous catalysts and applications. Chemosphere. 2017;189:224-38.
- [10] Gasim MF, Gooi Q-S, Oh WD. Peroxymonosulfate activation using CoFe2O4/Fe2O3 nanocomposite for Acid Orange removal. Journal of Applied Materials and Technology. 2023;3(2):34-43.
- [11] Ma J, Sui M-H, Chen Z-L, Wang L-N. Degradation of refractory organic pollutants by catalytic ozonation—activated carbon and Mn-loaded activated carbon as catalysts. Ozone: Science and Engineering. 2004;26 (1):3-10.
- [12] Prawiranegara A, Sugesti H, Utama PS, Saputra E. Mn/Carbon Sphere Catalyst For Heterogeneous Activation Of Peroxymonosulfate For Methylene Blue Removal. Chemica: Jurnal Teknik Kimia. 2021;8 No. 2 88-92.
- [13] Wang Y, Sun H, Ang HM, Tadé MO, Wang S. Synthesis of magnetic core/shell carbon nanosphere supported manganese catalysts for oxidation of organics in water by peroxymonosulfate. Journal of colloid and interface science. 2014;433:68-75.
- [14] Yan J, Fan Z, Wei T, Cheng J, Shao B, Wang K, et al. Carbon nanotube/MnO2 composites synthesized by microwave-assisted method for supercapacitors with high power and energy densities. Journal of Power Sources. 2009;194(2):1202-7.
- [15] Luo Y, Kong D, Luo J, Chen S, Zhang D, Qiu K, et al. Hierarchical TiO2 nanobelts@MnO2 ultrathin nanoflakes core–shell array electrode materials for supercapacitors. RSC Advances. 2013;3(34):14413-22.
- [16] Zhang X, Sun X, Zhang H, Zhang D, Ma Y. Microwave -assisted reflux rapid synthesis of MnO2 nanostructures and their application in supercapacitors. Electrochimica Acta. 2013;87:637-44
- [17] Saputra E, Zhang H, Liu Q, Sun H, Wang S. Eggshaped core/shell α-Mn2O3@ α-MnO2 as

- heterogeneous catalysts for decomposition of phenolics in aqueous solutions. Chemosphere. 2016;159:351-8.
- [18] Saputra E, Muhammad S, Sun H, Ang HM, Tadé MO, Wang S. Different Crystallographic One-dimensional MnO2 Nanomaterials and Their Superior Performance in Catalytic Phenol Degradation. Environmental Science & Technology. 2013;47 (11):5882-7.
- [19] Saputra E, Pinem JA, Budihardjo MA, Utama PS, Wang S. Carbon-supported manganese for heterogeneous activation of peroxymonosulfate for the decomposition of phenol in aqueous solutions. Materials Today Chemistry. 2020;16:100268.
- [20] Saputra E, Muhammad S, Sun H, Patel A, Shukla P, Zhu ZH, et al. α-MnO2 activation of peroxymonosulfate for catalytic phenol degradation in aqueous solutions. Catalysis Communications. 2012;26:144-8.
- [21] Yang J-CE, Yuan B, Cui H-J, Wang S, Fu M-L. Modulating oxone-MnOx/silica catalytic systems towards ibuprofen degradation: Insights into system effects, reaction kinetics and mechanisms. Applied Catalysis B: Environmental. 2017;205:327-39.
- [22] Utama PS, Widayatno WB, Azhar MR, Abid HR, Peng W, Muraza O, et al. LaMnO3 Perovskite Activation of Peroxymonosulfate for Catalytic Palm Oil Mill Secondary Effluent Degradation. Journal of Applied Materials and Technology. 2020;2(1):27-35.
- [23] Saputra E, Muhammad S, Sun H, Ang H-M, Tadé MO, Wang S. Manganese oxides at different oxidation states for heterogeneous activation of peroxymonosulfate for phenol degradation in aqueous solutions. Applied Catalysis B: Environmental. 2013;142:729-35.
- [24] Rauf M, Ashraf SS. Fundamental principles and application of heterogeneous photocatalytic degradation of dyes in solution. Chemical engineering journal. 2009;151(1-3):10-8.
- [25] Ghanbari F, Moradi M. Application of peroxymonosulfate and its activation methods for degradation of environmental organic pollutants. Chemical Engineering Journal. 2017;310:41-62.
- [26] Liu Y, Guo H, Zhang Y, Tang W, Cheng X, Liu H. Activation of peroxymonosulfate by BiVO4 under visible light for degradation of Rhodamine B. Chemical Physics Letters. 2016;653:101-7.
- [27] Saputra E, Prawiranegara BA, Nugraha MW, Oh W-D, Sugesti H, Utama PS. 3D N-doped carbon derived from zeolitic imidazole framework as heterogeneous catalysts for decomposition of pulp and paper mill effluent: Optimization and kinetics study. Environmental Research. 2023:116441.
- [28] Wang D, Luo X, Yang S, Xue G. Tourmaline/ Perovskite composite material as heterogeneous catalysts for activation peroxymonosulfate to remove organic dye in water. Journal of Environmental Chemical Engineering. 2021;9(3):105221.

- [29] Gong C, Chen F, Yang Q, Luo K, Yao F, Wang S, et al. Heterogeneous activation of peroxymonosulfate by Fe -Co layered doubled hydroxide for efficient catalytic degradation of Rhoadmine B. Chemical engineering journal. 2017;321:222-32.
- [30] Jiang L, Zhang Y, Zhou M, Liang L, Li K. Oxidation of Rhodamine B by persulfate activated with porous carbon aerogel through a non-radical mechanism. Journal of hazardous materials. 2018;358:53-61.



This article is licensed under a Creative Commons Attriution 4.0 International License.